Probing Real-Space and Time-Resolved Correlation Functions with Many-Body Ramsey Interferometry

Michael Knap,[1,2,*] Adrian Kantian,[3] Thierry Giamarchi,[3] Immanuel Bloch,[4,5] Mikhail D. Lukin,[1] and Eugene Demler[1]

[1]*Department of Physics, Harvard University, Cambridge, Massachusetts 02138, USA*
[2]*ITAMP, Harvard-Smithsonian Center for Astrophysics, Cambridge, Massachusetts 02138, USA*
[3]*DPMC-MaNEP, University of Geneva, 24 Quai Ernest-Ansermet CH-1211 Geneva, Switzerland*
[4]*Max-Planck-Institut für Quantenoptik, Hans-Kopfermann-Straße 1, 85748 Garching, Germany*
[5]*Fakultät für Physik, Ludwig-Maximilians-Universität München, 80799 München, Germany*

(Received 2 July 2013; revised manuscript received 18 September 2013; published 4 October 2013)

We propose to use Ramsey interferometry and single-site addressability, available in synthetic matter such as cold atoms or trapped ions, to measure real-space and time-resolved spin correlation functions. These correlation functions directly probe the excitations of the system, which makes it possible to characterize the underlying many-body states. Moreover, they contain valuable information about phase transitions where they exhibit scale invariance. We also discuss experimental imperfections and show that a spin-echo protocol can be used to cancel slow fluctuations in the magnetic field. We explicitly consider examples of the two-dimensional, antiferromagnetic Heisenberg model and the one-dimensional, long-range transverse field Ising model to illustrate the technique.

DOI: 10.1103/PhysRevLett.111.147205 PACS numbers: 75.10.Jm, 37.10.Ty, 47.70.Nd, 67.85.−d

In condensed matter systems, there exists a common framework for understanding such diverse probes as neutron and x-ray scattering, electron energy loss spectroscopy, optical conductivity, scanning tunneling microscopy, and angle-resolved photoemission. All of these techniques can be understood in terms of dynamical response functions, which are Fourier transformations of retarded Green's functions [1]

$$G^{AB,\mp}_{\mathrm{ret}}(t) := -\frac{i\theta(t)}{Z}\sum_n e^{-\beta E_n}\langle n|B(t)A(0) \mp A(0)B(t)|n\rangle. \tag{1}$$

Here, the summation goes over all many-body eigenstates $|n\rangle$, $\beta = 1/k_B T$, the partition function $Z = \sum_n e^{-\beta E_n}$, operators are given in the Heisenberg representation $A(t) = e^{i\hat{H}t}Ae^{-i\hat{H}t}$ ($\hbar$ is set to one in this Letter), signs $-$ $(+)$ correspond to commutator (anticommutator) Green's functions, and $\theta(t)$ is the Heaviside function. Correlation functions provide a direct probe of many-body excitations and their weight, describe many-body states, and give particularly important information about quantum phase transitions, where they exhibit characteristic scaling forms [2].

In the past few years, the experimental realization of many-body systems with ultracold atoms [3], polar molecules [4], and ion chains [5] has opened new directions for exploring quantum dynamics. However, most dynamical studies of such "synthetic matter" correspond to quench or ramp experiments: The initial state is prepared, then it undergoes some nontrivial evolution $|\Psi(t)\rangle = T_t e^{-i\int_0^t dt'\hat{H}(t')}|\Psi(0)\rangle$, and some observable A is measured $\langle A(t)\rangle = \langle\Psi(t)|A|\Psi(t)\rangle$. These experiments provide an exciting new direction for exploring many-body dynamics, but they do not give direct information about excitations of many-body systems as contained in dynamical response functions. Notable exceptions are phase or amplitude shaking of the optical lattice (see, e.g., [6–8], and references therein) and radio frequency spectroscopy [9], which can be understood as measuring the single-particle spectral function (i.e., the imaginary part of the corresponding response function). However, these techniques cannot be extended to measuring other types of correlation functions, such as spin correlation functions in magnetic states as realized in optical lattices or ion chains, and are often carried out in a regime far beyond linear response, which would be required to relate the measurement to theory within Kubo formalism [1].

In this Letter, we demonstrate that a combination of Ramsey interference experiments and single-site addressability available in ultracold atoms and ion chains can be used to measure real-space and time-resolved spin correlation functions; see Fig. 1 for an illustration of the

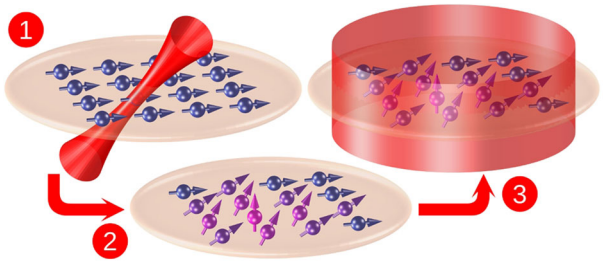

FIG. 1 (color online). Many-body Ramsey interferometry consists of the following steps: (1) A spin system prepared in its ground state is locally excited by $\pi/2$ rotation; (2) the system evolves in time; (3) a global $\pi/2$ rotation is applied, followed by the measurement of the spin state. This protocol provides the dynamic many-body Green's function.

protocol. This is in contrast to established condensed matter probes, which generally measure response functions in the frequency and wave vector domain. In principle, the two quantities are connected by Fourier transform, but the limited bandwidth of experiments renders a reliable mapping difficult in practice. We further discuss experimental limitations such as slow magnetic field fluctuations and show that global spin echo can be used to cancel these fluctuations.

Many-body Ramsey interference.—We consider a spin-1/2 system and introduce Pauli matrices σ_j^a for every site j with $a \in \{x, y, z\}$. At this point we do not make any assumptions on the specific form of the spin Hamiltonian. Examples will be given below. The internal states $|\downarrow\rangle_z$ and $|\uparrow\rangle_z$ of a single site j can be controlled by Rabi pulses which are of the general form [10,11]

$$R_j(\theta, \phi) = \hat{\mathbb{1}} \cos\frac{\theta}{2} + i(\sigma_j^x \cos\phi - \sigma_j^y \sin\phi) \sin\frac{\theta}{2}, \quad (2)$$

where $\theta = \Omega\tau$ with the Rabi frequency Ω and the pulse duration τ and ϕ is the phase of the laser field. For the many-body Ramsey interference we consider spin rotations with $\theta = \pi/2$ but ϕ arbitrary.

The many-body Ramsey protocol consists of four steps; see Fig. 1 for the first three of them: (1) perform a local $\pi/2$ rotation $R_i^1 := R_i(\pi/2, \phi_1)$ on site i; (2) evolve the system in time for a duration t; (3) perform a global (or local) $\pi/2$ spin rotation $R^2 := \prod_j R_j(\pi/2, \phi_2)$; and (4) measure σ^z on site j. The final measurement is destructive but can be carried out in parallel on all sites.

The result of this procedure, after repetition over many experimental runs, corresponds to the expectation value

$$M_{ij}(\phi_1, \phi_2, t) = \sum_n \frac{e^{-\beta E_n}}{Z} \langle n|R_i^\dagger(\phi_1) e^{i\hat{H}t} R^\dagger(\phi_2) \sigma_j^z R(\phi_2) e^{-i\hat{H}t} R_i(\phi_1)|n\rangle. \quad (3)$$

With some algebra we obtain [12]

$$M_{ij}(\phi_1, \phi_2, t) = \tfrac{1}{2}(\cos\phi_1 \sin\phi_2 G_{ij}^{xx,-} + \cos\phi_1 \cos\phi_2 G_{ij}^{xy,-} - \sin\phi_1 \sin\phi_2 G_{ij}^{yx,-} - \sin\phi_1 \cos\phi_2 G_{ij}^{yy,-}) + \text{terms with an odd number of } \sigma^{x,y} \text{ operators}, \quad (4)$$

where $G_{ij}^{ab,-}$ is the retarded, commutator Green's function defined in Eq. (1) with $A = \sigma_i^a$ and $B = \sigma_j^b$.

In many physically relevant models, terms with an odd number of σ operators vanish by symmetry or at least can be removed by an appropriate choice of the phases ϕ_1 and ϕ_2 of the laser fields. We show below when using these properties that in cases of both the Heisenberg model, Eq. (6), and the long-range, transverse field Ising model, Eq. (9), our Ramsey interference sequence measures a combination of retarded correlation functions

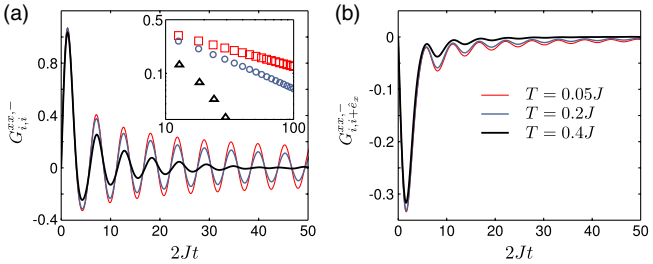

FIG. 2 (color online). Real-space and time-resolved Green's function $G_{ij}^{xx,-}$ of the two-dimensional, isotropic Heisenberg model, which can be measured with many-body Ramsey interferometry, shown for different temperatures T. The antiferromagnetic correlations manifest themselves in the opposite phase of on-site (a) and nearest-neighbor (b) correlations. The inset in (a) shows the decay of the peaks in $G_{ii}^{xx,-}$ on a double logarithmic scale. See the main text for details.

$$M_{ij}(\phi_1, \phi_2, t) = \frac{1}{4}\{\sin(\phi_1 + \phi_2)(G_{ij}^{xx,-} - G_{ij}^{yy,-}) - \sin(\phi_1 - \phi_2)(G_{ij}^{xx,-} + G_{ij}^{yy,-}) + \cos(\phi_1 + \phi_2)(G_{ij}^{xy,-} + G_{ij}^{yx,-}) + \cos(\phi_1 - \phi_2)(G_{ij}^{xy,-} - G_{ij}^{yx,-})\}. \quad (5)$$

Alternatively to the many-body Ramsey protocol, a spin-shelving technique can be used to measure dynamic spin correlations along the quantization direction; i.e., the operators A and B in (1) are σ_i^z and σ_j^z, respectively [12]. In Supplemental Material [12], we also derive a useful relation between Green's functions and the Loschmidt echo and discuss that it can be used to characterize diffusive and localized many-body phases.

Heisenberg model.—The anisotropic Heisenberg model of the XXZ type can be realized both with two-component mixtures [13–18] and with polar molecules [21–23] in optical lattices

$$\hat{H}_{\text{Heis}} = \sum_{i<j} J_{ij}^\perp(\sigma_i^x \sigma_j^x + \sigma_i^y \sigma_j^y) + J_{ij}^z \sigma_i^z \sigma_j^z. \quad (6)$$

For two-component Bose mixtures, interactions can be mediated through the superexchange mechanism, and $J_{ij}^\perp$ and J_{ij}^z are functions of the inter- and intraspecies scattering lengths, respectively, which are nonzero for i, j nearest neighbors. When realizing the Heisenberg model with polar molecules, $J_{ij}^\perp$ and J_{ij}^z are long ranged and anisotropic in space. Hamiltonian (6) is introduced for arbitrary dimension and the site index i is understood as a collective index. We assume that the system is prepared in equilibrium at finite temperature; i.e., it has a density matrix given by $\rho = Z^{-1} e^{-\beta \hat{H}_{\text{Heis}}}$.

Hamiltonian (6) has the global symmetry $\sigma^x \to -\sigma^x$, $\sigma^y \to -\sigma^y$, and $\sigma^z \to \sigma^z$, from which it is obvious that expectation values with an odd number of $\sigma^{x,y}$ vanish. In addition, Hamiltonian (6) has a U(1) symmetry of spin rotations around the z axis. This symmetry requires that

$$G_{ij}^{xx} - G_{ij}^{yy} = 0 \quad \text{and} \quad G_{ij}^{xy} + G_{ij}^{yx} = 0.$$

Hence, the many-body Ramsey protocol (5) measures

$$M_{ij}(\phi_1, \phi_2, t) = -\frac{1}{4}\{\sin(\phi_1 - \phi_2)(G_{ij}^{xx} + G_{ij}^{yy}) - \cos(\phi_1 - \phi_2)(G_{ij}^{xy} - G_{ij}^{yx})\}. \quad (7)$$

The choice of the phases ϕ_1 and ϕ_2 of the laser fields determines which combination of Green's functions is obtained.

In case the two spin states are not encoded in magnetic-field-insensitive states, one may also need to take into account fluctuating magnetic fields for a realistic measurement scenario. Such a contribution is described by a Zeeman term $\hat{H}_Z = h_z \sum_i \sigma_i^z$. A spin-echo sequence, however, which augments the Ramsey protocol with a global π rotation R^π after half of the time evolution, removes slow fluctuations in the Zeeman field

$$R(\phi_2)e^{-i(\hat{H}_{\text{Heis}}+\hat{H}_Z)(t/2)}R^\pi e^{-i(\hat{H}_{\text{Heis}}+\hat{H}_Z)(t/2)}R_i(\phi_1) \rightarrow \tilde{R}(\phi_2)e^{-i\hat{H}_{\text{Heis}}t}R_i(\phi_1), \quad (8)$$

where $\tilde{R}(\phi_2) = iR(\phi_2)(\cos\phi_\pi \prod_l \sigma_l^x - \sin\phi_\pi \prod_l \sigma_l^y)$ and ϕ_π is the phase of the laser field in the course of the π rotation. We show in Ref. [12] that this transformation still allows one to measure dynamic correlation functions.

Figure 2 shows the time-resolved, local (a) and nearest-neighbor (b) Green's function of the antiferromagnetic Heisenberg model ($J_{ij}^\perp = J_{ij}^z =: J$ for $i, j \in$ nearest neighbors and $J_{ij}^\perp = J_{ij}^z = 0$ otherwise) for different temperatures. We obtain the results by using a large-N expansion in Schwinger-Boson representation [24–26], which has been demonstrated to give reasonable results for the two-dimensional spin-1/2 Heisenberg antiferromagnet [27]. The local and nearest-neighbor, dynamic Green's functions show clear signatures of antiferromagnetic order, since their oscillations are out of phase. When lowering the temperature, the emergence of quantum coherence manifests through the increase in the amplitude of the oscillations. Furthermore, the decay of the oscillations [inset in (a)] follows at low temperatures a power law over several decades in time, which indicates the approach to criticality. The power law, however, is cut off by the finite correlation time $\log\tau \sim J/T$. Dynamic correlations at the antiferromagnetic ordering wave vector $\vec{\pi} := (\pi, \pi)$ are a precursor of long-range order [12] which in two dimensions emerges at zero temperature. These correlations can be obtained from the spatial ones by summing up contributions of one sublattice with positive sign and of the other with negative sign.

Long-range, transverse field Ising model.—Systems of trapped ions are capable of simulating canonical quantum spin models, where two internal states of the ions serve as effective spin states and the interaction between spins is mediated by collective vibrations [28,29]. Among the quantum spin models that can be simulated with trapped ions is the long-range, transverse field Ising model

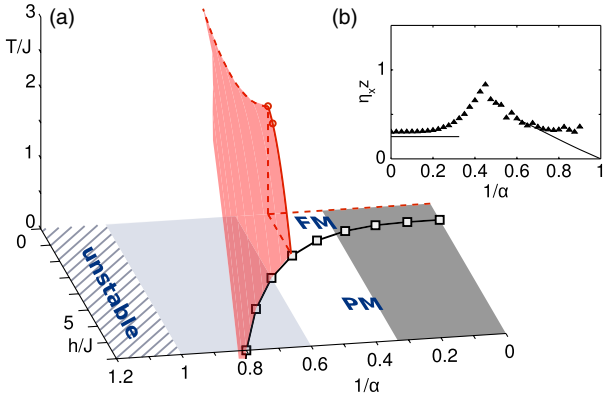

FIG. 3 (color online). Phase diagram (a) of the one-dimensional, long-range, transverse field Ising model (9) in the transverse field h, interaction exponent α, and temperature T space. For $\alpha < 1$ (hatched region), the system is thermodynamically unstable. The solid, black line indicates the quantum critical line, which separates the ferromagnetic (FM) and paramagnetic (PM) phases. For $\alpha > 3$ (dark gray region), the phase transition is of the same universality class as the short-range Ising transition; for $\alpha < 5/3$ (light gray region), mean-field analysis is exact [12]. At $\alpha = 2$ and $h = 0$ (dashed lines), the phase transition is of the Berezinskii-Kosterlitz-Thouless type [56–59], which also extends to finite transverse field h [39]. Symbols which indicate the finite temperature transition correspond to $h = 0$, $T = 1.5262(5)J$ [60] and $h = J/2$, $T = 1.42(1)J$ [61], which is in agreement with our results obtained with finite temperature Lanczos techniques [62,63]. (b) Critical exponent η_{xz} of dynamic correlations $G_{L/2,L/2}^{xx,-}(t)$ obtained along the critical line from the scaling of finite size systems, which are realizable in current experiments (symbols) and exact results in the thermodynamic limit (lines).

$$\hat{H}_{\text{Ising}} = -\sum_{i<j} J_{ij}\sigma_i^x\sigma_j^x - h\sum_i \sigma_i^y, \quad (9)$$

where the spin-spin interactions fall off approximately as a power law $J_{ij} = J/|i-j|^\alpha$ with exponent α and h is the strength of the transverse field. In trapped ion systems, power-law interactions can be engineered with an exponent α that is highly tunable [28]. The upper limit of α is given by the decay of dipolar interactions $0 < \alpha < 3$; however, the shorter ranged the interactions are, the slower the overall time scales are, which in turn is challenging for experiments.

Experimentally, the long-ranged Ising model has been realized with ion chains for both FM $J > 0$ [30,31] as well as antiferromagnetic $J < 0$ [32–38] coupling. Theoretically, quantum spin systems with long-range interactions that decay with arbitrary exponent α have rarely been studied in the literature, and so far static properties [39–42] and quantum quenches [43–45] have been explored. This is why we discuss the one-dimensional, ferromagnetic ($J > 0$), long-range, transverse-field Ising model in greater detail and focus in particular on dynamical correlation functions and on the quantum phase transition (QPT) from the FM to the PM phase, whose universality is described by a continuous manifold of

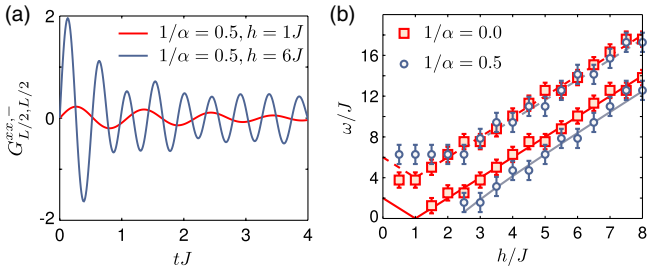

FIG. 4 (color online). Dynamic Green's function $G^{xx,-}_{L/2,L/2}(t)$ (a) of the long-range, transverse field Ising model (9) for interaction exponent $\alpha = 2$ in the ferromagnetic ($h = J$) and in the paramagnetic ($h = 6J$) phases; see the legend. (b) Oscillation frequencies (symbols) in $G^{xx,-}_{L/2,L/2}(t)$ obtained from a Fourier transform of the time-dependent data as a function of the transverse field h for two different values of the interaction exponent α. Error bars indicate the resolution of the Fourier transform in frequency space. Solid lines illustrate the excitation gap, and the dashed line the upper band edge, which defines the oscillations contributing to the dynamic correlations.

critical exponents that can be tuned by the decay of the interactions α; see Fig. 3(a) for the rich phase diagram.

The transverse field Ising model obeys the global symmetry $\sigma^x \to -\sigma^x$, $\sigma^y \to \sigma^y$, and $\sigma^z \to -\sigma^z$, and thus only expectation values with an odd number of σ^x operators vanish in Eq. (5). However, when choosing the phases $\phi_1 = 0$ and $\phi_2 = \pi/2$ it can be shown that the many-body Ramsey protocol measures [12]

$$M_{ij}(0, \pi/2, t) = \frac{1}{2} G^{xx,-}_{ij}. \tag{10}$$

We illustrate that insight into the many-body physics can be obtained by studying systems which are currently experimentally realizable. To this end, we solve systems of up to 22 ions with exact diagonalization based on the Lanczos technique [46] and calculate their dynamical Green's functions. As realized in experiments, we generally consider open boundary conditions. In Fig. 4(a), we show dynamic Green's functions $G^{xx,-}_{L/2,L/2}$ for the interaction exponent $\alpha = 2$ in the FM and in the PM phase. The time-resolved Green's functions characterize the many-body states: In the FM phase (h smaller than the critical field h_c that determines the QPT) the response in the direction of the ferromagnet is small, which manifests in $G^{xx,-}_{L/2,L/2}$ through small amplitude oscillations whose envelope decays very slowly, whereas in the PM phase ($h > h_c$) the response is large, which in $G^{xx,-}_{L/2,L/2}$ manifests in oscillations that initially have a large amplitude but decay quickly in time.

The oscillations in the dynamic Green's functions contain information about the excitations in the system. In particular, in the PM phase oscillations with a frequency corresponding to the gap [2] are expected. In addition, the spectrum is cut off due to the lattice, which gives rise to a second energy scale present in both the PM and the FM phase. In Fig. 4(b), we show the frequency components extracted from the Fourier transform of $G^{xx,-}_{L/2,L/2}(t)$ with error bars given by the resolution in frequency space for both short-ranged interactions ($1/\alpha = 0$, squares) and long-ranged interactions ($1/\alpha = 1/2$, circles). For short-range interactions $1/\alpha = 0$, the gap can be evaluated analytically $\Delta = 2|h - J|$ [2], which grows linearly with the transverse field as indicated by the solid red (dark) line in Fig. 4(b). The upper band edge at $\Delta + 4J$ is indicated by the dashed red (dark) line. At the critical point $h_c = J$, the gap closes; however, oscillations from the finite bandwidth are still present. For long-ranged interactions, we extract the excitation gap and the bandwidth numerically. Results are shown by blue (light) solid and dashed lines, respectively. The upper band edge [blue (light) dashed line] almost coincides with the short-range system. The gap and the upper band edge are in good agreement with the frequency components extracted from the correlation functions.

Along the quantum critical line $h = h_c(\alpha)$, which can be determined experimentally by measuring, for example, the Binder ratio [47], the system becomes scale invariant, and thus spatial and temporal correlations decay as power laws [see Fig. 3(b)]. In Ref. [12], we show in detail that a change in the critical exponents should be observable in current experiments already with a medium number of ions.

Conclusions and outlook.—In summary, we proposed a protocol to measure real-space and time-resolved spin correlation functions by using many-body Ramsey interference. We discuss the protocol for two relevant examples of the Heisenberg and the long-range transverse field Ising model, which can be experimentally realized with cold atoms, polar molecules, and trapped ions. In this work we focused on spin-1/2 systems. However, the proposed protocol can be generalized to higher-spin systems when realizing the Rabi pulses (2) with the respective higher-spin operators. In order to implement the generalized spin rotations, spin states should be encoded in internal atomic states with isotropic energy spacing which can be simultaneously addressed by Rabi pulses.

The measurement of the time-dependent Green's functions provides important information on many-body excitations and on quantum phase transitions where they exhibit specific scaling laws. Having such tools at hand makes it possible to explore fundamental, theoretically much debated many-body phenomena. In particular, we believe that the many-body localization transition [48–50] and many-body localized phases, which are characterized by a dephasing time that grows exponentially with the distance between two particles in the sample [51–53], can be explored by using the ideas described in this work.

Another question is whether the many-body Ramsey protocol can be applied to systems out of equilibrium. The protocol we propose is based on discrete symmetries of many-body eigenstates and thus holds for ensembles described by diagonal density matrices, while a generic

system out of equilibrium is characterized by a density matrix which also contains off-diagonal elements. However, if the off-diagonal elements dephase in time, many-body Ramsey interferometry can be applied out of equilibrium as well. This could, for example, also be the case for integrable systems, which after fast dephasing are described by a diagonal density matrix whose weights are determined by the generalized Gibbs ensemble [54,55].

We thank S. Gopalakrishnan, R. Islam, C. Monroe, and S. Sachdev for useful discussions. The authors acknowledge support from Harvard-MIT CUA, the DARPA OLE program, AFOSR MURI on Ultracold Molecules, ARO-MURI on Atomtronics, the Austrian Science Fund (FWF) Project No. J 3361-N20, as well as the Swiss NSF under MaNEP and Division II. T. G. is grateful to the Harvard Physics Department and to Harvard-MIT CUA for support and hospitality during the completion of this work. Numerical calculations have been performed on the Odyssey cluster at Harvard University Research Computing.

*knap@physics.harvard.edu

[1] A. L. Fetter and J. D. Walecka, *Quantum Theory of Many-Particle Systems* (McGraw-Hill, New York, 1971).
[2] S. Sachdev, *Quantum Phase Transitions* (Cambridge University Press, Cambridge, England, 2011), 2nd ed.
[3] I. Bloch, J. Dalibard, and W. Zwerger, Rev. Mod. Phys. **80**, 885 (2008).
[4] T. Lahaye, C. Menotti, L. Santos, M. Lewenstein, and T. Pfau, Rep. Prog. Phys. **72**, 126401 (2009).
[5] R. Blatt and C. F. Roos, Nat. Phys. **8**, 277 (2012).
[6] C. Kollath, A. Iucci, T. Giamarchi, W. Hofstetter, and U. Schollwöck, Phys. Rev. Lett. **97**, 050402 (2006).
[7] A. Tokuno and T. Giamarchi, Phys. Rev. Lett. **106**, 205301 (2011).
[8] M. Endres, T. Fukuhara, D. Pekker, M. Cheneau, P. Schauß, C. Gross, E. Demler, S. Kuhr, and I. Bloch, Nature (London) **487**, 454 (2012).
[9] J. T. Stewart, J. P. Gaebler, and D. S. Jin, Nature (London) **454**, 744 (2008).
[10] M. A. Nielsen and I. L. Chuang, *Quantum Computation and Quantum Information* (Cambridge University Press, Cambridge, England, 2000).
[11] H. Häffner, C. Roos, and R. Blatt, Phys. Rep. **469**, 155 (2008).
[12] See Supplemental Material at http://link.aps.org/supplemental/10.1103/PhysRevLett.111.147205 for details on the interferometric protocols, the dynamic signature of long-range order in the Heisenberg antiferromagnet, and the quantum phase transition of the long-range, transverse field Ising model.
[13] A. M. Rey, V. Gritsev, I. Bloch, E. Demler, and M. D. Lukin, Phys. Rev. Lett. **99**, 140601 (2007).
[14] S. Trotzky, P. Cheinet, S. Fölling, M. Feld, U. Schnorrberger, A. M. Rey, A. Polkovnikov, E. A. Demler, M. D. Lukin, and I. Bloch, Science **319**, 295 (2008).
[15] S. Nascimbène, Y.-A. Chen, M. Atala, M. Aidelsburger, S. Trotzky, B. Paredes, and I. Bloch, Phys. Rev. Lett. **108**, 205301 (2012).
[16] T. Fukuhara, A. Kantian, M. Endres, M. Cheneau, P. Schauß, S. Hild, D. Bellem, U. Schollwöck, T. Giamarchi, C. Gross, I. Bloch, and S. Kuhr, Nat. Phys. **9**, 235 (2013).
[17] D. Greif, T. Uehlinger, G. Jotzu, L. Tarruell, and T. Esslinger, Science **340**, 1307 (2013).
[18] The short-range, transverse field Ising model [19] as well as frustrated classical magnetism [20] have also been explored with cold atoms.
[19] J. Simon, W. S. Bakr, R. Ma, M. E. Tai, P. M. Preiss, and M. Greiner, Nature (London) **472**, 307 (2011).
[20] J. Struck, C. Ölschläger, R. L. Targat, P. Soltan-Panahi, A. Eckardt, M. Lewenstein, P. Windpassinger, and K. Sengstock, Science **333**, 996 (2011).
[21] A. V. Gorshkov, S. R. Manmana, G. Chen, J. Ye, E. Demler, M. D. Lukin, and A. M. Rey, Phys. Rev. Lett. **107**, 115301 (2011).
[22] A. V. Gorshkov, S. R. Manmana, G. Chen, E. Demler, M. D. Lukin, and A. M. Rey, Phys. Rev. A **84**, 033619 (2011).
[23] B. Yan, S. A. Moses, B. Gadway, J. P. Covey, K. R. A. Hazzard, A. M. Rey, D. S. Jin, and J. Ye, Nature (London) **501**, 521 (2013).
[24] D. P. Arovas and A. Auerbach, Phys. Rev. B **38**, 316 (1988).
[25] A. Auerbach and D. P. Arovas, Phys. Rev. Lett. **61**, 617 (1988).
[26] A. Auerbach, *Interacting Electrons and Quantum Magnetism* (Springer, New York, 1994).
[27] E. Manousakis, Rev. Mod. Phys. **63**, 1 (1991).
[28] D. Porras and J. I. Cirac, Phys. Rev. Lett. **92**, 207901 (2004).
[29] X.-L. Deng, D. Porras, and J. I. Cirac, Phys. Rev. A **72**, 063407 (2005).
[30] A. Friedenauer, H. Schmitz, J. T. Glueckert, D. Porras, and T. Schaetz, Nat. Phys. **4**, 757 (2008).
[31] R. Islam, E. Edwards, K. Kim, S. Korenblit, C. Noh, H. Carmichael, G.-D. Lin, L.-M. Duan, C.-C. Joseph Wang, J. Freericks, and C. Monroe, Nat. Commun. **2**, 377 (2011).
[32] K. Kim, M.-S. Chang, R. Islam, S. Korenblit, L.-M. Duan, and C. Monroe, Phys. Rev. Lett. **103**, 120502 (2009).
[33] K. Kim, M.-S. Chang, S. Korenblit, R. Islam, E. E. Edwards, J. K. Freericks, G.-D. Lin, L.-M. Duan, and C. Monroe, Nature (London) **465**, 590 (2010).
[34] E. E. Edwards, S. Korenblit, K. Kim, R. Islam, M.-S. Chang, J. K. Freericks, G.-D. Lin, L.-M. Duan, and C. Monroe, Phys. Rev. B **82**, 060412(R) (2010).
[35] B. P. Lanyon, C. Hempel, D. Nigg, M. Müller, R. Gerritsma, F. Zähringer, P. Schindler, J. T. Barreiro, M. Rambach, G. Kirchmair, M. Hennrich, P. Zoller, R. Blatt, and C. F. Roos, Science **334**, 57 (2011).
[36] J. W. Britton, B. C. Sawyer, A. C. Keith, C.-C. J. Wang, J. K. Freericks, H. Uys, M. J. Biercuk, and J. J. Bollinger, Nature (London) **484**, 489 (2012).
[37] R. Islam, C. Senko, W. C. Campbell, S. Korenblit, J. Smith, A. Lee, E. E. Edwards, C.-C. J. Wang, J. K. Freericks, and C. Monroe, Science **340**, 583 (2013).
[38] P. Richerme, C. Senko, S. Korenblit, J. Smith, A. Lee, R. Islam, W. C. Campbell, and C. Monroe, Phys. Rev. Lett. **111**, 100506 (2013).

[39] A. Dutta and J. K. Bhattacharjee, Phys. Rev. B **64**, 184106 (2001).
[40] N. Laflorencie, I. Affleck, and M. Berciu, J. Stat. Mech. (2005) P12001.
[41] A. W. Sandvik, Phys. Rev. Lett. **104**, 137204 (2010).
[42] T. Koffel, M. Lewenstein, and L. Tagliacozzo, Phys. Rev. Lett. **109**, 267203 (2012).
[43] M. L. Wall and L. D. Carr, New J. Phys. **14**, 125015 (2012).
[44] P. Hauke and L. Tagliacozzo, arXiv:1304.7725.
[45] J. Schachenmayer, B. P. Lanyon, C. F. Roos, and A. J. Daley, Phys. Rev. X **3**, 031015 (2013).
[46] Y. Saad, *Numerical Methods for Large Eigenvalue Problems* (Manchester University, Manchester, England, 1995).
[47] K. Binder, Phys. Rev. Lett. **47**, 693 (1981).
[48] D. Basko, I. Aleiner, and B. Altshuler, Ann. Phys. (N.Y.) **321**, 1126 (2006).
[49] I. V. Gornyi, A. D. Mirlin, and D. G. Polyakov, Phys. Rev. Lett. **95**, 206603 (2005).
[50] V. Oganesyan and D. A. Huse, Phys. Rev. B **75**, 155111 (2007).
[51] M. Serbyn, Z. Papić, and D. A. Abanin, Phys. Rev. Lett. **110**, 260601 (2013).
[52] D. A. Huse and V. Oganesyan, arXiv:1305.4915.
[53] M. Serbyn, Z. Papić, and D. A. Abanin, Phys. Rev. Lett. **111**, 127201 (2013).
[54] M. Rigol, V. Dunjko, V. Yurovsky, and M. Olshanii, Phys. Rev. Lett. **98**, 050405 (2007).
[55] M. Rigol, V. Dunjko, and M. Olshanii, Nature (London) **452**, 854 (2008).
[56] D. J. Thouless, Phys. Rev. **187**, 732 (1969).
[57] J. M. Kosterlitz, Phys. Rev. Lett. **37**, 1577 (1976).
[58] J. L. Cardy, J. Phys. A **14**, 1407 (1981).
[59] J. Bhattacharjee, S. Chakravarty, J. L. Richardson, and D. J. Scalapino, Phys. Rev. B **24**, 3862 (1981).
[60] E. Luijten and H. Meßingfeld, Phys. Rev. Lett. **86**, 5305 (2001).
[61] A. W. Sandvik, Phys. Rev. E **68**, 056701 (2003).
[62] J. Jaklič and P. Prelovšek, Phys. Rev. B **49**, 5065 (1994).
[63] M. Aichhorn, M. Daghofer, H. G. Evertz, and W. von der Linden, Phys. Rev. B **67**, 161103(R) (2003).